CHAPTER-3

Study of bioactivity of V_2O_5 substituted

Borosilicate glass system

3.1 Introduction:

Bioactive glass is an innovative material for about 40 years. It started to take off commercially in the past ten years. Bioglass has a property to develop new properties after enhancing its components. When a substance called bioactive glass gets absorbed into the body, it reacts with bodily fluids to kill bacteria, stimulate cells, and help repair tissues at the same time [1-2]. Borosilicate glass having a chemical composition of SiO_2 (74%), Na_2O (16 %), and B_2O_3 (10%), was invented by Otto Schott [3]. Borosilicate glass has the ability to attach to bone without any fibrous tissue at the contact. At the implant's contact with bodily fluid, the ion exchange produces an alkaline pH (>7) that promotes the crystallization and nucleation process of a carbonate apatite layer, which is chemically and physically identical to the bone mineral composition. The Glass begin to dissolve due to the body's reaction with it, and the liberated ions may have both an antibacterial and a cell-recruiting impact. And so, along with the material acting as a scaffold for the cells to attach and grow [4]. Hydroxyapatite, which was formed on the surface, found an inorganic component of bone. So, these bioactive glasses are being used as a substitute for bone. However, Bioactive glass is being used in the modern world to trigger bone formation and tunnable degradability, which is better than other bioceramic materials [9]. There is much research done on different glasses in the case of their electrical properties [10-13] and their bioactivity [14-18]. Many studies were done on various properties of transition metal-containing glasses [6,8]. Borosilicate bioactive glasses are also widely used with other materials doping across the world [24,31]. Vanadium doped borosilicate glass luminescence property studied [33]. Vanadium (V) oxide (formula -V_2O_5) is an inorganic compound that is an amphoteric oxide, i.e., it can be acidic as well as basic. Among the vanadium compounds, vanadium pentoxide (V_2O_5) is the most stable form of oxidized vanadium, which has the largest electron storage capacity per unit. So, it could be a factor in its catalytic behaviour, which contributes to its bioactivity. The oxygen atoms in its structure

also enable the production of receptive oxygen species. The development of V2O5 was facilitated by its exceptional stability and low degradation rate, which enabled its use in long-term applications. So, we have selected vanadium here due to its therapeutic action. It is known to enhance early wound healing, which may be of particular use in situations involving diabetes individuals and the healing of soft tissues. V_2O_5 was also utilized to cover the surface of implants and is characterized as a bioactive substance [7]. Their addition to borosilicate glass is also helpful in nuclear disposal [26]. In the present study, V_2O_5 is used as a substitution material in Borosilicate glass. Vanadium (V) oxide exhibits very acute toxicity in human bodies. So we are using vanadium in less amount, i.e., up to 4 % only. Being toxic, we used V_2O_5 as its cellular compatibility obtained was very high. Hemocompatibility of these bioactive glasses is carried out with human blood with the help of PBS and Triton X-100 [22,23]. Its bone cell compatibility is studied with the help of MG-63 cell lines for orthopaedic applications [28-30]. However, its poor mechanical and electrical parameters limit our application, i.e. monolithic [27]. Electrical properties of the sample are incorporated with its electrical properties HCP is an infix material used for orthopaedic applications. Various research work found that natural bone is piezoelectric in nature [10,11]. So here, the SBF immersed sample exhibits improved electrical properties [25], which help in bone metabolism. Vanadium pentaoxide improves bioactivity, which plays a crucial role in the human body. Hence, the current investigation was conducted to examine the role of V_2O_5 in borosilicate glasses.

3.2 Experiment procedure:

Materials and Synthesis of Bioactive glass:

A bioactive borosilicate glass with the substitution of vanadium pentaoxide named VBG is being prepared by conventional melt quenching method. The glasses are made in packs of 100 grams by combining the specified constituents of borosilicate glass, as shown in Table 3.1. The batches were subjected to melting in platinum crucibles inside a globar furnace at a

temperature of 1400ºC, followed by holding for 2 hrs. The molten liquid is carefully poured into rectangular stainless steel molds that have been preheated and have dimensions of 1cmx1cmx4cm. The glass samples, after that, promptly moved to an annealed muffle furnace, which is kept at 500ºC for annealing. Following that, it is gradually cooled at a pace of 30ºC per hour until it reaches room temperature. Then, the glass undergoes fragmentation into smaller fragments and is then transformed into a powdered state using the ball milling procedure. Certain pallets undergo compression to assess the electrical, physical, and mechanical qualities of the specimen. The SBF solution is being made using the established approach developed by Kokubo et al. [9]. The powdered sample is immersed into SBF then the samples was used for conducting in-vitro analysis of the sample. The osteosarcoma cell line MG-63 [5] used to assess the compatibility of samples cell line and human blood used to determine the hemocompatibility.

Table 3.1 Weight % composition of V_2O_5 substituted bioactive glass.

Sample	**SiO_2**	**Na_2O**	**B_2O_3**	**V_2O_5**
V1	74	16	10	0
V2	73.9	16	10	0.1
V3	73.7	16	10	0.3
V4	73.5	16	10	0.5
V5	73	16	10	1
V6	71.5	16	10	2.5
V7	70	16	10	4

3.3 Characterization

3.3.1 Density, Molar Volume, and Mechanical Properties:

The determination of the molar volume, and the glass density of bioactive borosilicate glass samples is achieved using following formula:

Density calculation formula:

$$\rho = \left[\frac{Wa}{\{Wa - Wb\}}\right] \rho_b \ (g/cm^3) \qquad \text{.....(1)}$$

Molar volume calculation formula:

$$Vm = \frac{M}{\rho}(cm^3) \qquad (2)$$

Where W is the atomic weight and *M* is the molar mass of our prepared glass samples.

To determine the density of a glass sample, it is necessary to get a little piece of material and immerse it in a suitable soaking medium such as xylene. To assess the compressive strength, the powdered sample underwent uniaxial pressing using a hydraulic press at a pressure of 12 tons for 70 seconds. This process led to the creation of a pallet body with dimensions of 10×2 mm^2. The pallets are subjected to a sintering process at 800°C for 4 hours, with a heating and cooling rate of the furnace set at 4°C per minute. The measurement of compressive strength is conducted with a Universal Testing Machine (UTM). The pH values of the samples immersed in SBF solution were assessed at regular intervals of 2, 7, 14, 21, and 28 days. The fluctuation in the pH values is used to ascertain the chemical properties of the bioglass samples.

3.3.2 The *in-vitro* bioactivity analysis:

Biological Characterization involves assessing the bioactivity of samples by subjecting them to immersion in a solution known as Simulated Body Fluid (SBF) for varying durations. The preparation of the SBF solution is carried out according to the specifications explained by Kokubo et al 2006. The powdered sample is maintained in a bottle with the SBF solution, with a consistent ratio of 1:100 between the model and the solution. Subsequently, pH values were measured at 2, 7, 14, 21, and 28 days. Following each designated period, the SBF solution was discarded, and the material underwent a drying procedure in an oven kept at the temperature about 70°C for a minimum duration of 7 hours. Subsequently, samples were transferred to an

incubator at 37°C for further processing. All samples undergo a drying process, after drying these samples are subjected to analysis using an XRD, FTIR, SEM and EDX testing techniques. All these techniques are used to identify the HCA layer deposition over the surface of bioactive glass samples.

XRD: The X-ray diffraction analysis (XRD) method is used to determine the crystallographic structure of a given sample. To analyze the X-ray diffraction pattern of the produced bioactive glass samples, we used the Rigaku Desktop Miniflex II X-ray diffractometer. The sample was in powder form and was subjected to characterization. Cu-Kα radiation and a Ni filter were employed throughout the analysis process. XRD analysis was conducted within a 2θ range from 10° to 80°, with a step duration of 2 seconds and a step size 0.02. In materials research, an item is exposed to incident X-rays as part of an X-ray diffractometer (XRD) examination. Following this exposure, the intensity and diffraction angles of the emitted X-rays that depart the object are then measured. XRD analysis is used to examine the diffraction pattern of X-rays to determine the composition of the substance under investigation.

FTIR: The Fourier Transform Infrared spectroscopy (FTIR) technique is used to ascertain the development of chemical bonds inside the substance [21]. The JASCO FTIR 4600 Fourier Transform Infrared Spectrometer (FTIR) instrument was used within the spectral region of 400-2000 cm-1 to investigate sample alterations before and after immersion in SBF solution.

SEM-EDS: The Scanning Electron Microscope (SEM) technology is used to ascertain the morphology that exists inside a compound. The morphological examination of materials before and after immersion in SBF solution is determined using the instrument EVO-MA15/18, (USA) at 10µm. Using this instrument, we analysed EDX (Energy-Dispersive X-ray Spectroscopy) analysis of the samples to determine the elements present in the samples. In

this study, we examine the creation of a Hydroxy apatite layer on the sample by analyzing its constituent components.

Electrical Property: Pallets of 1 cm diameter and 1 mm thickness are prepared and sintered at 800C to measure the dielectric property of the samples.

3.3.3 *In-vitro* Hemocompatibility:

In this procedure, the blood compatibility of the substance is assessed with human blood, as indicated by prior research conducted [23]. Initially, human blood is obtained from the median cubital veins using heparin-coated tubes, which serve as an anticoagulant. A centrifugation process was conducted at a force of 650 g for 10 minutes at a temperature of 4ºC. Subsequently, the supernatant was meticulously discarded. The red blood cell pellets were washed until the supernatant was clarified. Later, the blood was diluted with phosphate-buffered saline (PBS) at 1:10 (blood to PBS). Following this, a suspension of red blood cells (RBCs) measuring 0.1 ml was combined with a product concentration of 1 mg/ml (in PBS) measuring 0.9 ml. Phosphate-buffered saline (PBS) has a pH of 7.4 and demonstrates no discernible lysis value. Triton X-100 serves as a positive control, indicating complete lysis at a rate of 100%. The combined products were placed in a shaker incubator at 37 ± 1 ℃ for 1 hour, with continuous stirring. Subsequently, the mixture was centrifuged with a force of 650 g for 10 minutes at a temperature of 4ºC. This centrifugation step separated the non-lysed red blood cells from the other components. The optical density at 540nm of the supernatant was determined using a microplate reader to assess its lysis.

$$\textbf{Heamolysis} = \frac{\textbf{ODsample} - \textbf{OD0}}{\textbf{OD100} - \textbf{OD0}} \textbf{ X 100}$$

Where, OD samples, OD100 and OD0 are the optical density (OD) of the samples, positive control (Triton-X, 100% hemolysis) and negative control (PBS, 0% hemolysis), respectively [22-23].

3.3.4 Cellular Compatibility:

The technique involves the assessment of various biological events within particular cellular contexts, leading to the identification of possible confounding factors that manifest in organisms. In this study, we proceed to examine the samples that have been previously prepared. The cell culture procedure facilitates the assessment of bioactivity. The cell proliferation and cell viability of the specimen are assessed using the MG-63 cell line, a representative model of human bone cells. The activity development of the MG-63 cell line was assessed over a period of about 48 hours using various compositions.

I. **Cell line maintenance:** The MG-63 cell line, a widely used cell line in scientific research, was incubated in a controlled environment in a humidified CO_2 incubator at a temperature of 37 °C. The cells were cultured in DMEM, supplemented with FBS (Fetal Bovine Serum). To further protect against microbial contamination and maintain the sterility of the culture, penicillin-streptomycin solution was added [29]. This carefully controlled environment and nutrient-rich medium provide optimal conditions for the growth and propagation of the MG-63 cells.

II. **Cellular compatibility assay**: The effect of V_2O_5 substitution borosilicate glass samples (Base, 0.1%, 0.3%, 0.5%, 2.5% and 4%) has been examined for cellular proliferation of MG-63 cell line by MTT assay. For this, 10,000 cells were seeded in each well of 96-well cell culture plate and allowed to adhere overnight. V_2O_5 substituted borosilicate glass samples were suspended in 1ml of PBS at a stock concentration of 5 mg/ml. The cells were incubated for 24 hours after being exposed to various concentration (100µg/ml, 200 µg/ml, 400µg/ml, 600 µg/ml, 800 µg/ml) [24]. Following removing the media from each well, MTT-containing medium was added to each well. After 2 hours of incubation, the MTT-containing medium was removed, and

then each well received 100 µl of DMSO. Thereafter, the wells underwent another 30 minutes of incubation. The measurement of absorbance was conducted at a wavelength of 570 nm with a multiplate reader. [24].

III. **Phase contrast Imaging:** The proliferation of MG-63 cell line has been observed *in-vitro* live cell imaging by phase contrast microscope. In brief, MDA-MB-231 cells were seeded at a density of 1 x 105 cells per well on 12-well tissue culture plates. The plates were then placed in an incubator set at a temperature of 37˚C and a 5% CO_2 humidified atmosphere for a duration of 24 hours. The cells were exposed with V_2O_5 substituted borosilicate glass samples at concentration (100µg/ml, 200 µg/ml, 400µg/ml, 600 µg/ml, 800 µg/ml) [24]. After 24 hrs of treatment, images were taken under inverted phase contrast microscope (EVOS FL cell imaging system, Life Technologies, USA) at 100x magnification.

3.3.5 Electrical Property:

The dielectric property of the samples is measured [32]. base borosilicate glass sample exhibits a white colour. However, an increase in V_2O_5 doping results in the glass acquiring a greenish colour. As the concentration of V_2O_5 doping is raised, the green colour becomes darker. The powder crushed in mortar with the help of pestle. The pellets were produced using a hydraulic press with a force of 8 tonnes in a die with 1 cm diameter and 1 mm thickness. The resulting pellets was then subjected to heating cycles at a temperature of 850°C for 5 hours each, resulting in the formation of a compact pellet. Subsequently, emery paper of a fine grain size was used to refine the pellet's surface. Subsequently, the application of silver paste on both sides of the pellet was conducted for electroding. Later, the shots were subjected to a heat treatment at a temperature of 300°C for one hour, intending to facilitate the drying process. The impedance spectroscopy investigation of the pellets was conducted using

a Metrohm Autolab (PGSTAT204) equipped with a FRA32M module. The analysis of the impedance data was performed using the NOVA software.

Table 3.2 Chemical composition, molar volume, density and compressive strength of glass samples.

Sample	Composition of samples, mole fraction value in %				Molar volume(cm^3) ±0.01	Density (g/cm^3) ± 0.003	Compressive strength (MPa)
	SiO_2	Na_2O	B_2O_3	V_2O_5			
V1	75.35	15.84	8.81	0.00	23.87	2.558	34.09
V2	75.3	15.86	8.82	0.03	23.88	2.561	58.26
V3	75.184	15.87	8.824	0.098	23.89	2.567	62.01
V4	75.138	15.899	8.84	0.169	23.93	2.568	71.69
V5	74.838	15.953	8.87	0.339	23.97	2.571	89.47
V6	74.065	16.12	8.96	0.853	24.12	2.582	103.77
V7	73.273	16.288	9.056	1.383	24.28	2.591	112.37

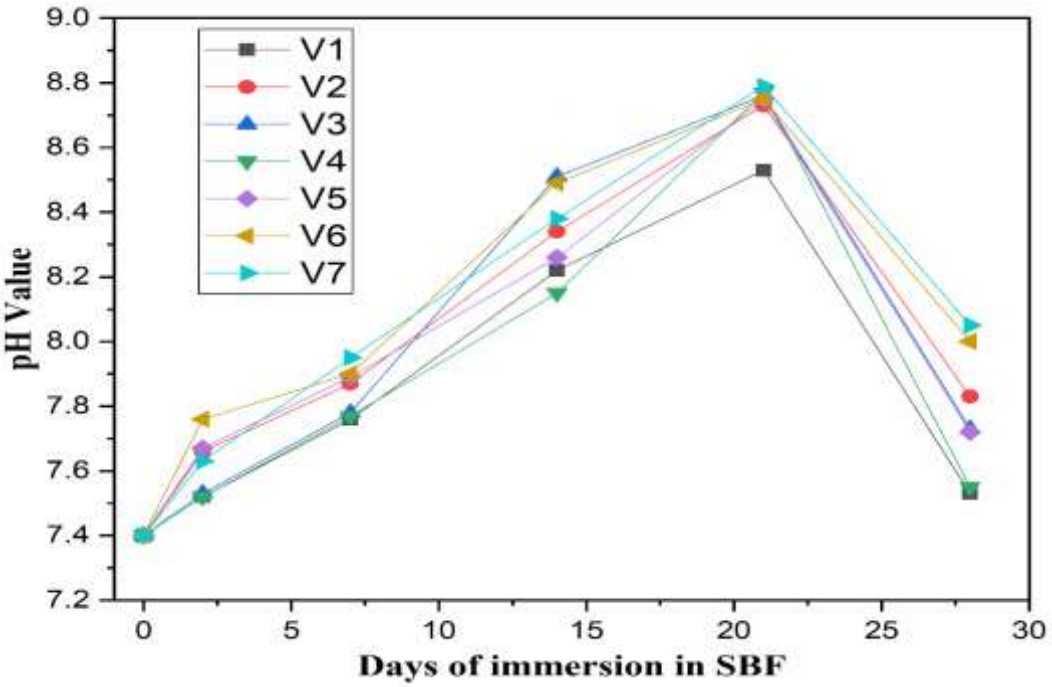

Figure 3.1 pH value variation after immersion in SBF for base and different V_2O_5 substituted borosilicate glass.

3.4 Results and Discussion

3.4.1 Physical, Chemical and Mechanical Properties:

The determination of the molar fraction and molar volume is facilitated with the use of equations 1 and 2. The molar volume exhibits an upward trend as the mole percentage of V_2O_5 rises. An experimental investigation was conducted to determine the density and compressive strength of borosilicate glasses, both base and substituted with V_2O_5. Pellets were made for this purpose. The data presented in Table 3.2 demonstrates an advantageous correlation between the content of V_2O_5 and the density of the glasses. The replacement of SiO_2 with V_2O_5 results in an increase in density due to the latter's more compact structure. Increasing the compactness of samples contributes to the enhancement of their compressive strength. The compressive strength of the samples is also shown to be enhanced. This increased value exhibits more prominence in the context of bone contact. The samples exhibit enhanced strength and increased adaptability in the context of bone tissue bonding. It is well acknowledged that one of the primary drawbacks of hydroxyapatite (HA) is its mechanical qualities. However, efforts have been made to enhance these properties, hence mitigating the predefined limitations.

Following the immersion of the bioglass samples in SBF, the pH of the samples exhibited a rise, as seen in Figure 3.1. The pH value of the solution rose as a result of the elevated concentration of Na^+ alkali ions originating from the glass. The first step involves an ion exchange process in which sodium ions are replaced by the development of a layer of HA on the samples. However, after the production of HA is fully accomplished, the pH value begins to decrease. The chemical reaction achieves stability after the process of ion exchange has been fully executed. This provides us with an understanding of the time required for the sample to attain a state of stability. The bioactivity of HA formation stability is assessed by measuring the resulting outcomes.

3.4.2 XRD Phase analysis:

The base and substituted borosilicate glass was determined to be amorphous in nature. This result is obtained by the XRD seen in Figure 3.2(a). It shows only a bump formed between 20^o to 35^o (2 theta), which represents the presence of silica bonds (Si-O-Si) in the samples [15].

In Figure 3.2(b), we can see a sharp peak at 31.8^o (2 thetas), which represents the formation of $Ca_{10.042}$ $(PO_4)_{5.952}$ $(OH)_{2.292}$ (JCPDS code-2536) HAP bond in the base and substituted borosilicate glass samples which are immersed in SBF solution for 28 days. So here, the formation of the phosphate band is present after 28 days. This sharp peak shows the formation of HA. Another sharper peak is also present in the XRD of bioactive glasses containing 1 % V_2O_5, 2.5% V_2O_5, and 4% V_2O_5 substituted borosilicate glass samples. This sharp peak is present at 45.41^o (2 thetas), representing the formation of sodium phosphate bond, i.e. $Na_2(HPO)_4$ (code 7099), which releases phosphate bonds as studied from JCPDS data analysis [35]. So, these results indicate the formation of HA, i.e. bioactivity.

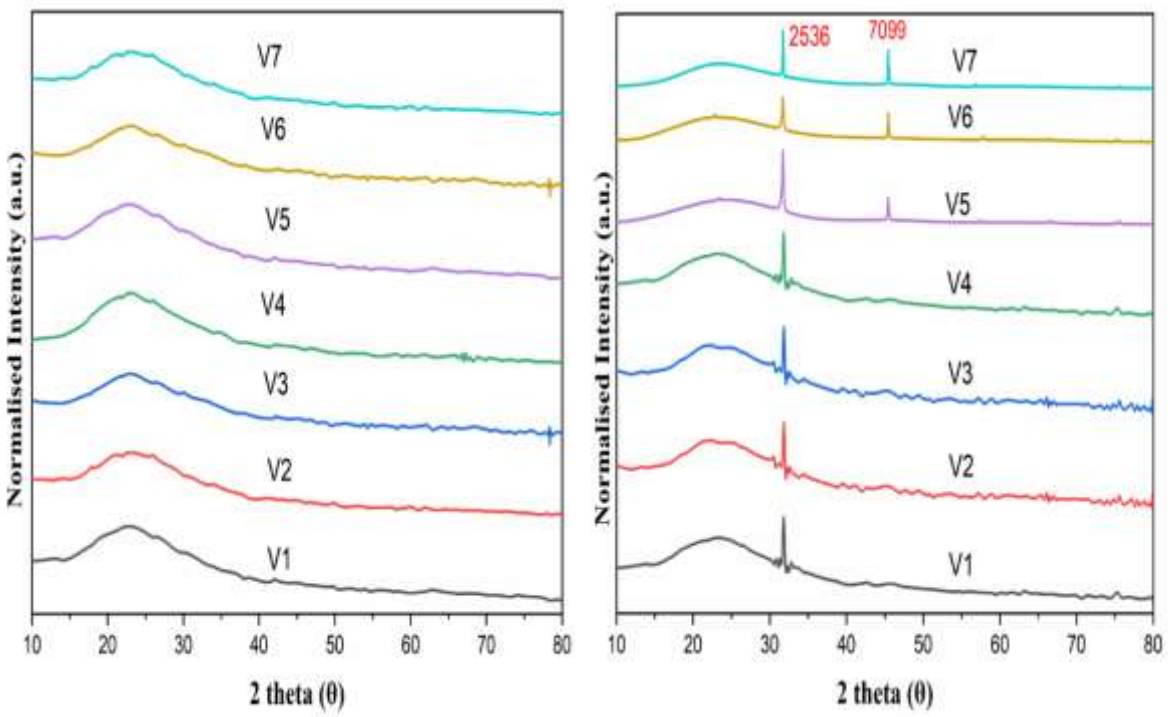

Figure 3.2 XRD graph for base and V_2O_5 substituted borosilicate samples **(a)** before and **(b)** after immersion in SBF solution.

3.4.3 FTIR Transmittance Analysis:

FTIR is used to check the functional group present in the bioactive borosilicate glass samples [21]. In Figure 3.3(a) shows the functional group i.e. Si-O bond, V-O bond and C=O bond formation. While in Figure 3.3(b) we can see the formation of the Si-O-Si (Band), Si-O-Si (Stretch), C-O (Stretch), P-O (Bend) and the presence of (hydroxyl) OH groups on the surface, which resulted favourably due to the formation of HA in respective samples after they have been immersed in the SBF solution for 28 days. 400-450 cm-1 (P-O bond), 450-550 (Si-O bond) cm^{-1} represents the formation of silica bonds. The peak around 788 cm^{-1} shows the V-O bond and 880 cm^{-1} to 1150cm^{-1} shows Si-O-Si bond stretch. Moreover, the peak range over 1180–1250 cm−1 (P-O bond) [19], 1330–1400 cm−1 (O-H bond) and 1600–1800 cm−1 (CO_3^{2-} bond) [20] obtained. The results we obtained indicate that the peaks corresponding to carbonyl, hydroxy, and P-O bonds becomes sharper as the level of V_2O_5 substitution increases. The findings demonstrate that the increase in V_2O_5 substitution in the borosilicate glass samples leads to increase of the HA layer over the surface of sample.

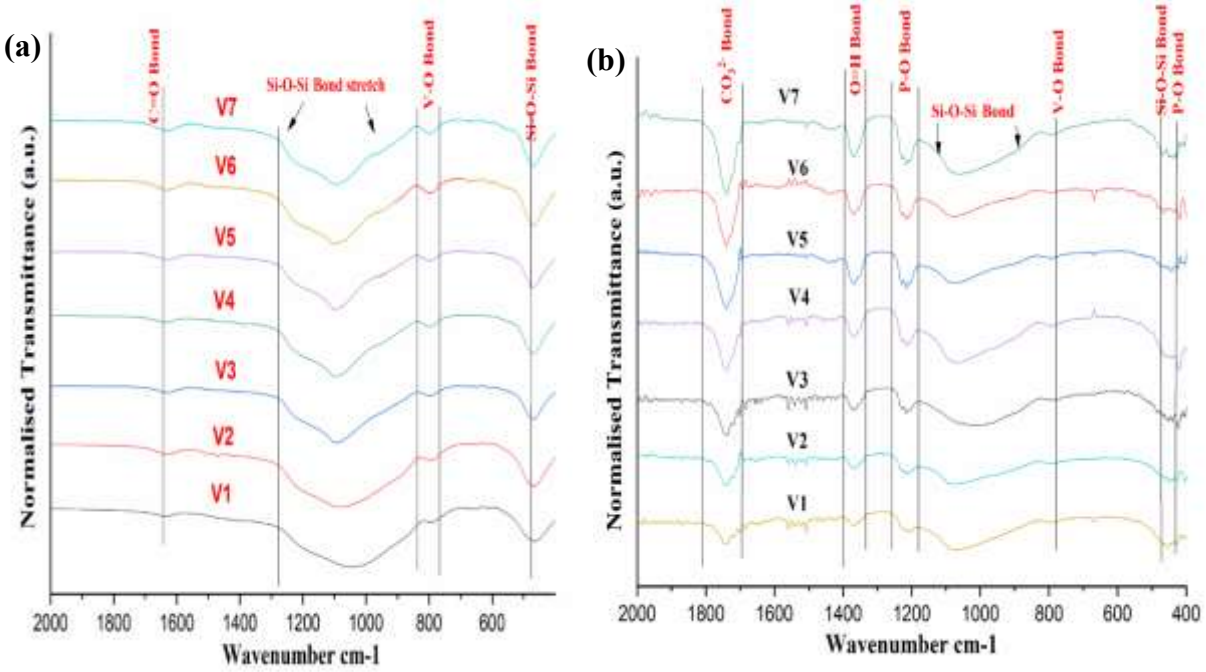

Figure 3.3 FTIR graph for base and V_2O_5 substituted borosilicate samples **(a)** before and **(b)** after 28 days of immersion in SBF.

3.4.4 SEM and EDS analysis:

The results obtained from the Scanning Electron Microscope (SEM) micrographs and EDS (Energy-Dispersive X-ray Spectroscopy) graph images are as follows: Figure 3.4.1, 3.4.2, 3.4.3, 3.4.4, 3.4.5, 3.4.6 and 3.4.7 shows results of base borosilicate glass, 0.1% V_2O_5, 0.3% V_2O_5, 0.5% V_2O_5, 1% V_2O_5, 2.5% V_2O_5 and 4% V_2O_5 respectively. In the SEM images taken before immersing the samples in SBF solution, no layer is seen above the samples. However, after immersing the samples in SBF solution for 28 days, white deposits can be seen on the surfaces of the samples. The presence of these white deposits on the surface indicates the creation of a hydroxyapatite layer [15-18]. The existence of a hydroxyapatite (HA) layer is confirmed by the corresponding EDS analysis, which is evident from the detection of calcium and phosphorus elements in the graph acquired after immersing in simulated bodily fluid (SBF). Our findings indicate that the increase of V_2O_5 doping in the borosilicate glass samples increases the white spots layer. This rise suggests the formation of a greater hydroxyapatite layer over the samples. The results demonstrate that the *in-vitro* bioactivity of the samples is enhanced with increasing levels of V_2O_5 doping in the borosilicate glass samples.

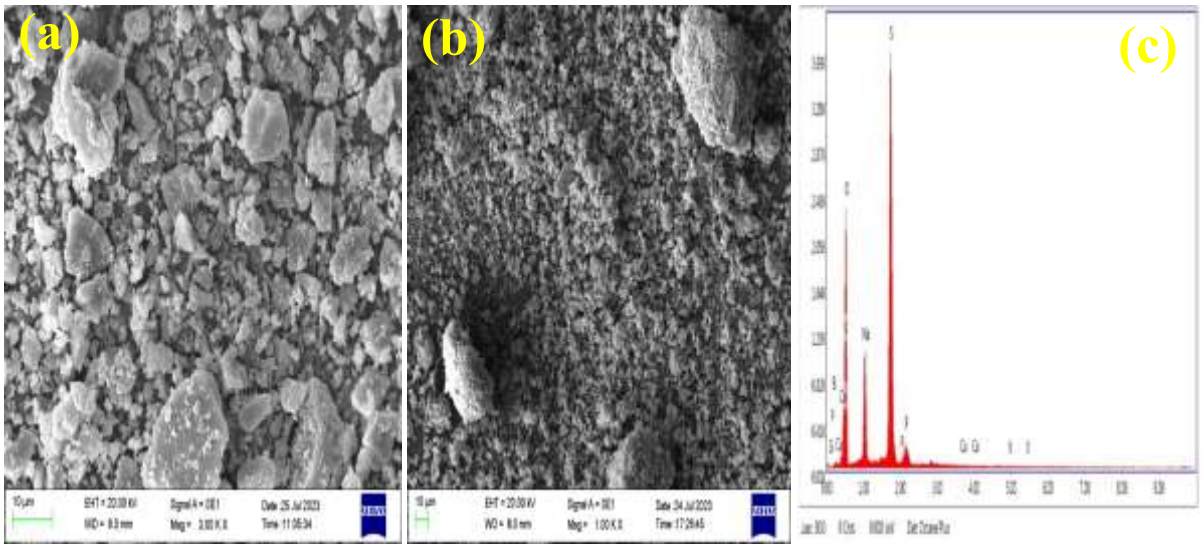

Figure 3.4.1 SEM-EDS image of base borosilicate glass samples **(a)** SEM image before SBF immersion **(b)** SEM image after 28 days immersion in SBF solution **(c)** EDS image after SBF immersion in SBF solution.

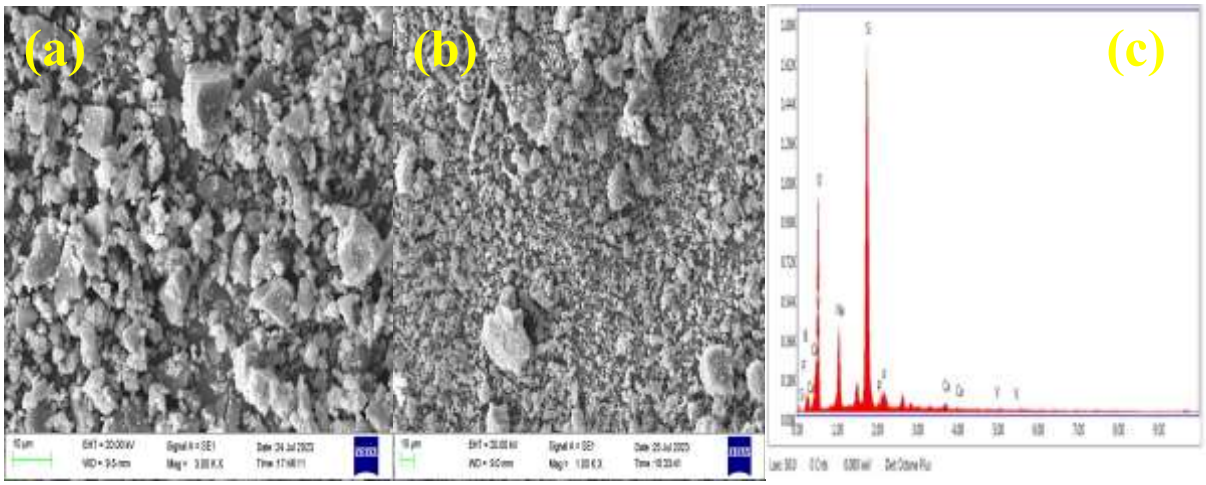

Figure 3.4.2 SEM-EDS image of 0.1% V_2O_5 substituted borosilicate glass samples **(a)** SEM image before SBF immersion **(b)** SEM image after 28 days immersion in SBF solution **(c)** EDS image after SBF immersion in SBF solution.

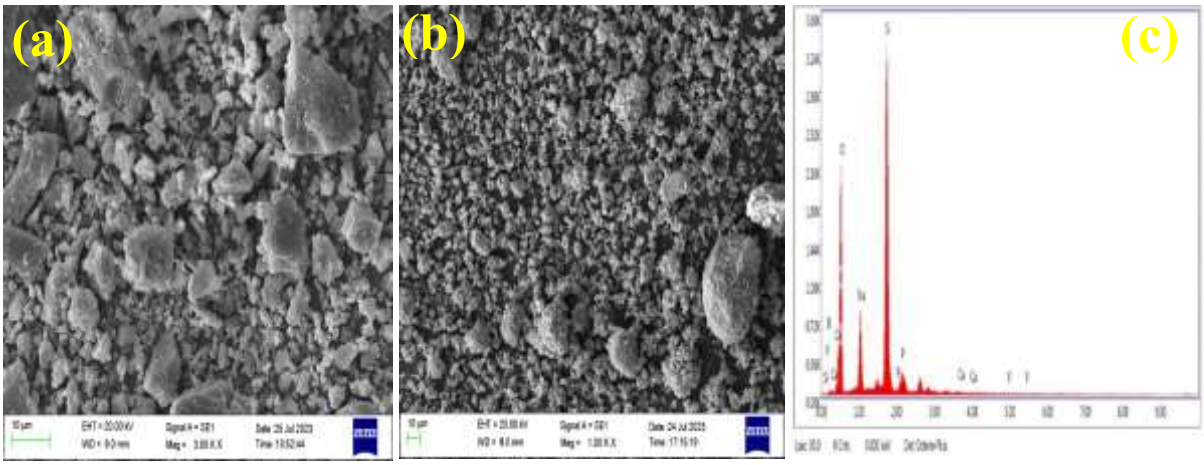

Figure 3.4.3 SEM-EDS image of 0.3% V_2O_5 substituted borosilicate glass samples **(a)** SEM image before SBF immersion **(b)** SEM image after 28 days immersion in SBF solution **(c)** EDS image after SBF immersion in SBF solution.

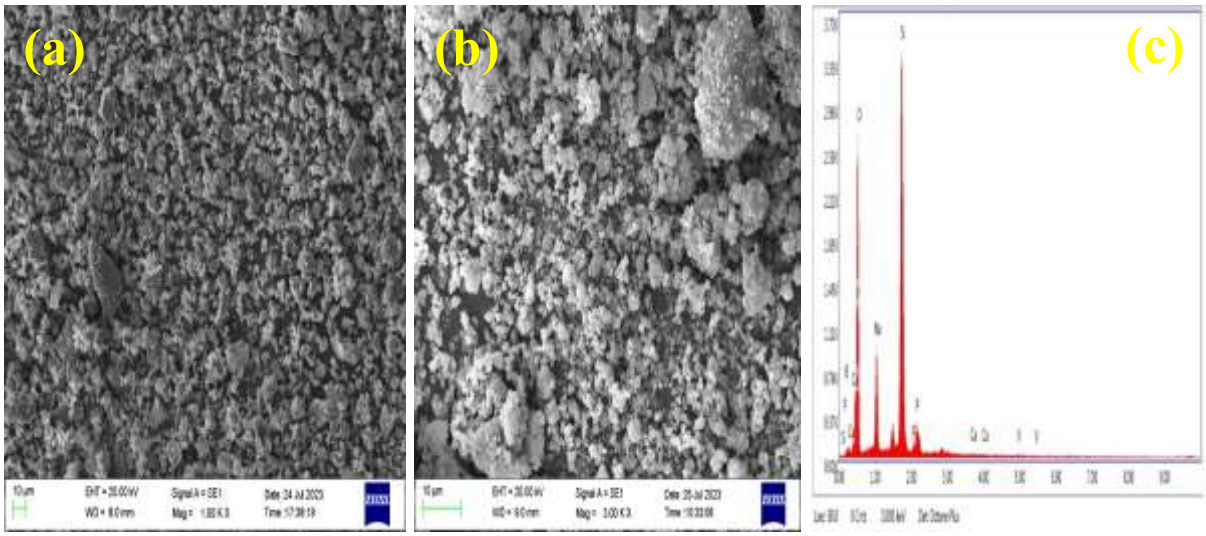

Figure 3.4.4 SEM-EDS image of 0.5% V_2O_5 substituted borosilicate glass samples **(a)** SEM image before SBF immersion **(b)** SEM image after 28 days immersion in SBF solution **(c)** EDS image after SBF immersion in SBF solution.

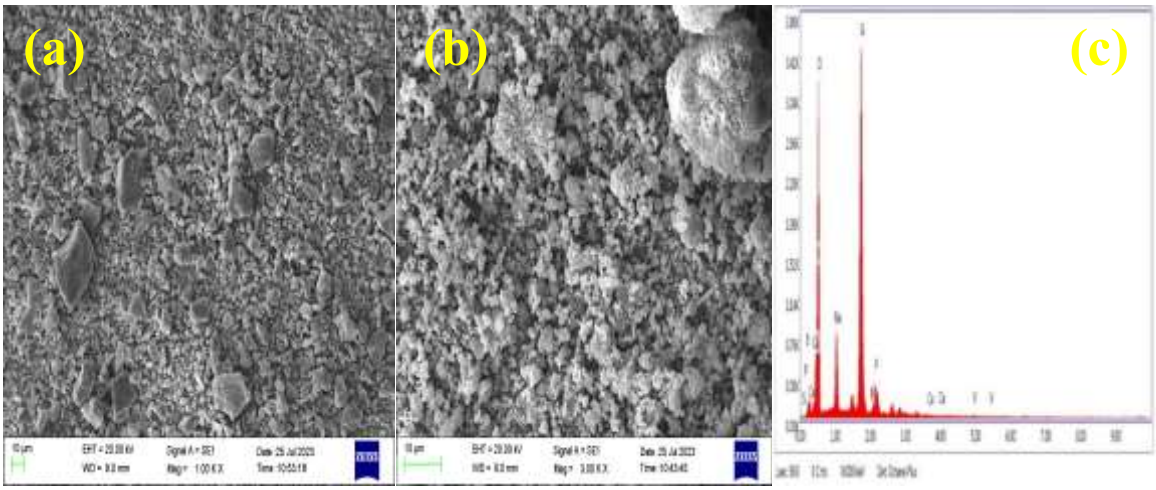

Figure 3.4.5 SEM/EDS image of 1% V_2O_5 substituted borosilicate glass samples **(a)** SEM image before SBF immersion **(b)** SEM image after 28 days immersion in SBF solution **(c)** EDS image after SBF immersion in SBF solution.

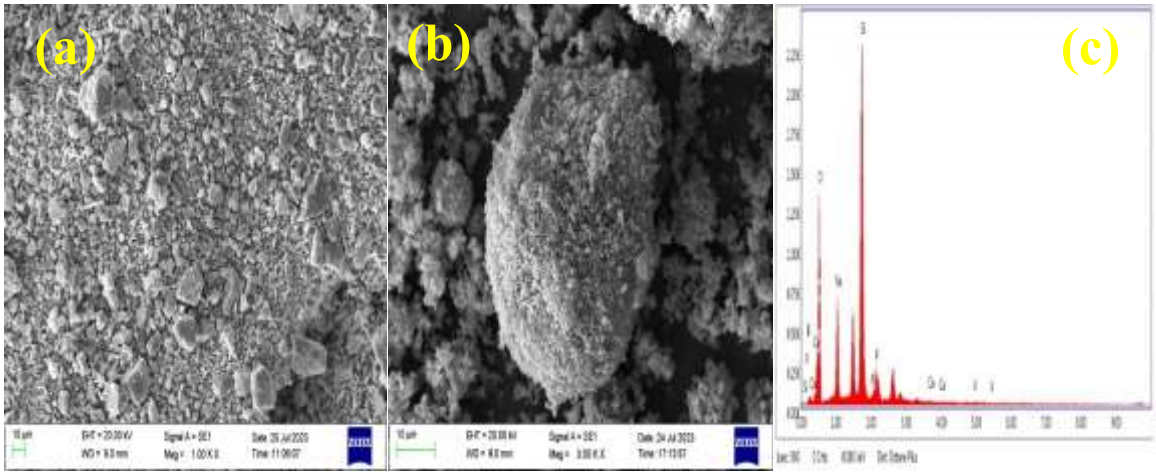

Figure 3.4.6 SEM-EDS image of 2.5% V_2O_5 substituted borosilicate glass samples **(a)** SEM image before SBF immersion **(b)** SEM image after 28 days immersion in SBF solution **(c)** EDS image after SBF immersion in SBF solution.

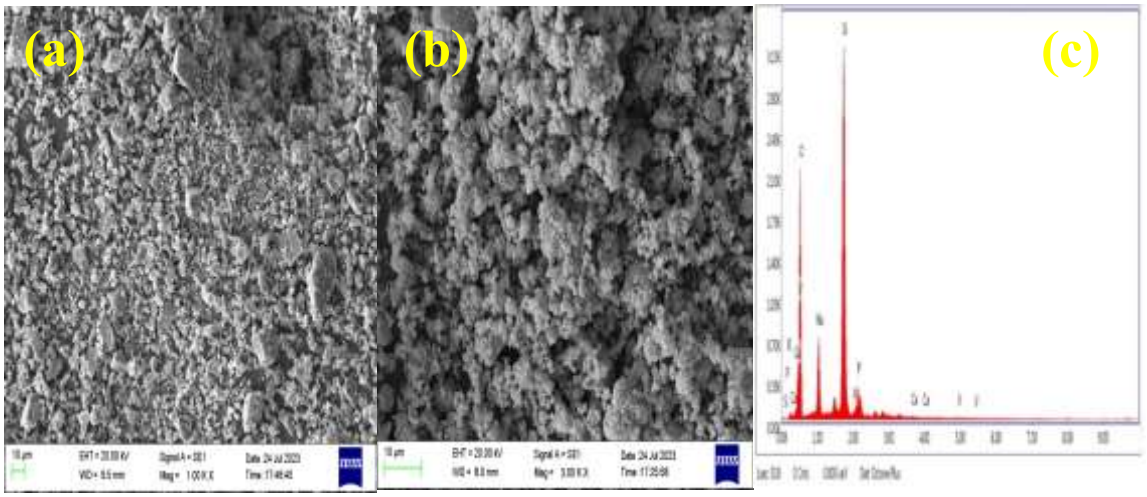

Figure 3.4.7 SEM-EDS image of 4% V_2O_5 substituted borosilicate glass samples **(a)** SEM image before SBF immersion **(b)** SEM image after 28 days immersion in SBF solution **(c)** EDS image after SBF immersion in SBF solution.

3.4.5 *In-vitro* Hemocompatibility:

In this study we found in the result that all samples are compatible with human blood. As shown in figure 3.5(A) we see here no lysis of blood samples is obtained. So we can say here that it is compatible with human blood. The products demonstrated less than 4% haemolysis in figure 3.5(B), which was significantly lower ($p < 0.01$) than the positive control group (triton x-100) reported to possess a significant haemolytic effect [22]. The developed products demonstrated favourable blood compatibility and were determined to be appropriate for administration.

[A]

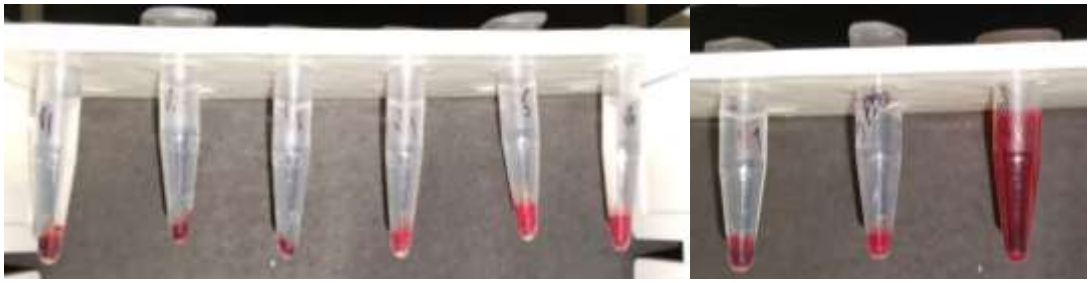

[B]

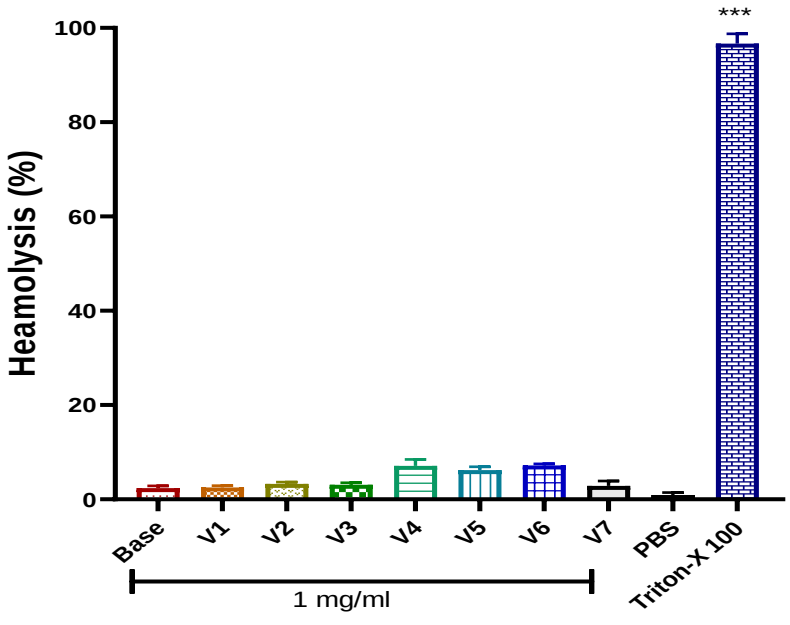

Figure 3.5 Ex vivo Hemocompatibility of the developed product; **(A)** represents the after haemolytic study, **(B)** % of haemolytic activity of different base and V_2O_5 substituted borosilicate samples.

3.4.6 The *In-vitro* Cellular Analysis:

In this study as shown in bar graph and images we found that all samples we obtained after V_2O_5 doping are biocompatible. In Diagram we can see that its proliferation value is increased up to 0.5% then the value is decreased after 4% V_2O_5 substituted.

I. **Cellular compatibility assay**: The V_2O_5 substituted borosilicate glass samples (0%, 0.1%, 0.3% and 0.5%) induced significant concentration-dependent proliferation on MG-63 cell line even at higher concentration however with 2.5% and 4% significant cytotoxicity were observed at the 600 µg/ml and 800 µg/ml concentrations. The proliferations of cells in the presence of the samples were shown in Fig 3.6.1. The statistical analysis was performed by One-way ANOVA followed by Tukey's test where * denotes significant difference (proliferation) at $p<0.05$ level compared to control and # denotes significant difference (inhibition) ($p<0.05$). Our results demonstrated that 0.5% V_2O_5 substituted borosilicate synthesized glass samples enhanced the ability of cells to survive and proliferate indicates a promising opportunity for bone repair. [24].

II. **Phase contrast Imaging:** The *in-vitro* imaging with phase contrast microscope revealed that with increase in concentration of V_2O_5 substituted borosilicate glass (100µg/ml, 200 µg/ml, 400µg/ml, 600 µg/ml, 800 µg/ml) the confluency of cell increases. Fig 3.6.2 depict maximum cell proliferation has been observed in 0.5% V_2O_5 substituted borosilicate glass sample at concentration 800 µg/ml. However, at the 600 µg/ml and 800 µg/ml concentrations of 2.5% and 4%, the confluency of MG-63 cell decreases. This further validate the result of MTT assay. Taken together, our results demonstrate that V_2O_5 substituted borosilicate glass has a significant application on bone regeneration.

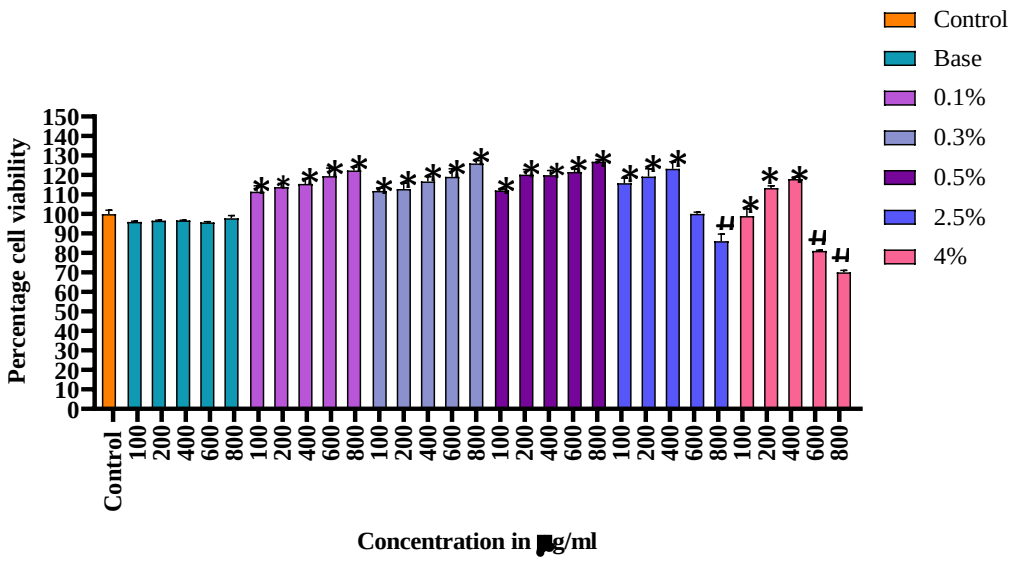

Figure 3.6.1 Cytotoxic investigations of V_2O_5 substituted borosilicate glass samples (Base, 0.1%, 0.3%,0.5%,2.5% and 4%) against MG-63 cell line.

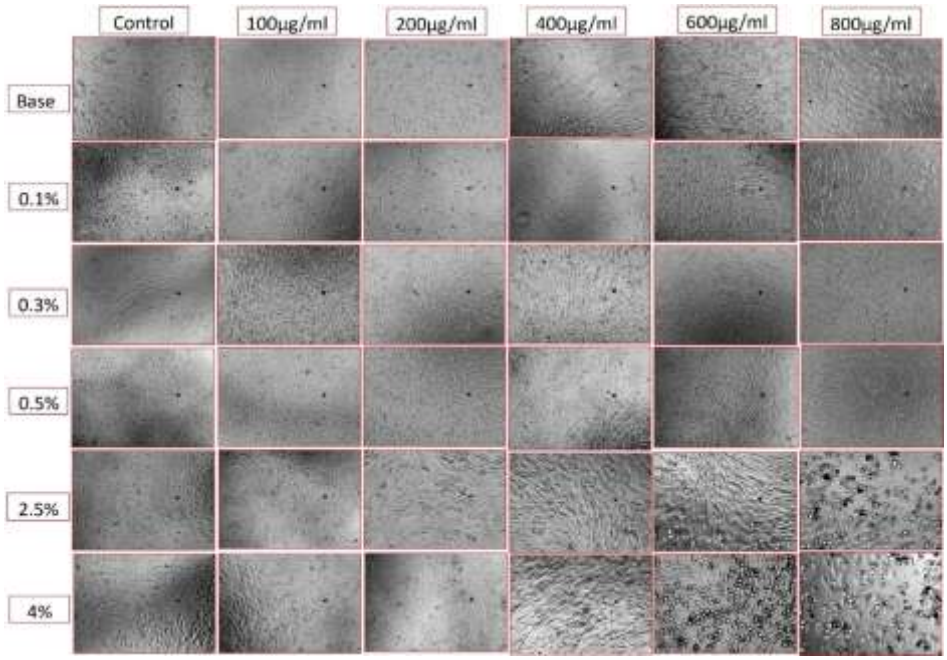

Figure 3.6.2 Phase contrast microscopic images of V_2O_5 substituted borosilicate glass samples (Base, 0.1%, 0.3%,0.5%,2.5% and 4%) against MG-63 cell line at different concentration showing proliferation of cells in concentration dependent manner except in 2.5% and 4%.

3.4.7 Electrical Properties:

It is widely acknowledged that the conduction process seen in silicate glasses mostly involves the movement of monovalent alkali ions down an ionic path. The monovalent alkali ions are located inside silicate glasses at interstitial places due to the splitting of the silicon-oxygen bonds. The monovalent alkali modifiers have a significant tendency for detachment

and migration, resulting in enhanced conduction. The reduction in ionic size of the alkali cation species further facilitates this conduction. The incorporation of divalent oxides into silicate glass has been found to enhance its chemical properties and reduce its conductivity. This phenomenon can be related to the obstruction or slowing down of the conduction pathways for monovalent alkali ions. This obstruction is caused by the presence of mixed cations with varying charges and the existence of other ions with larger ionic sizes, which in turn leads to lower ion mobility. [23].

I. **Before SBF:** The Figure 3.7(a) describe the changes in permittivity and Figure 3.8(a) shows dielectric loss of borosilicate glass with respect to frequency both in its pure form and when substituted with 2.5% V_2O_5. The tests were conducted within a frequency range spanning from 0Hz to 100kHz, at a temperature of 31°C. Figure 3.7(a) illustrate that anomalous dispersion is characterized by a slight reduction in the value of ε as the applied frequency increases. It is worth noting that the values of ε for the substituted samples exhibit a small increase compared to the base borosilicate samples over the whole range of investigated frequencies. Figure 3.8(a) shows the dependence of dielectric loss vs frequency applied to the samples under investigation. The dielectric loss values of V_2O_5 substituted glasses are greater than those of base borosilicate glass. This difference may be attributed to the increased conductivities resulting from including V_2O_5. In Figure 3.8(a), it is obvious that the dielectric loss values in the lower frequency range is more, suggesting the existence of direct current (dc) conductivity.

II. **After SBF:** Figure 3.7(b) shows the relationship between permittivity (ε), while Figure 3.8(b) illustrates the dielectric loss observed in the glasses under investigation after their immersion in SBF solution, as a function of frequency. The V_2O_5 substituted sample exhibits lower values of permittivity and dielectric loss in comparison to the base sample. The conduction inside and between V_2O_5 and the glass matrix experiences

increased limitations due to the formation of hydroxy apatite bonds on the surface of the matrix. Consequently, the resultant permittivity exhibited a decrease in comparison to the permittivity of glass that of base glass. Based on predictions, it is anticipated that the analyzed sample would exhibit a decreased dielectric loss compared to the base sample. This is attributed to the development of hydroxy apatite on the outer layer of the glass matrix in the presence of V_2O_5.

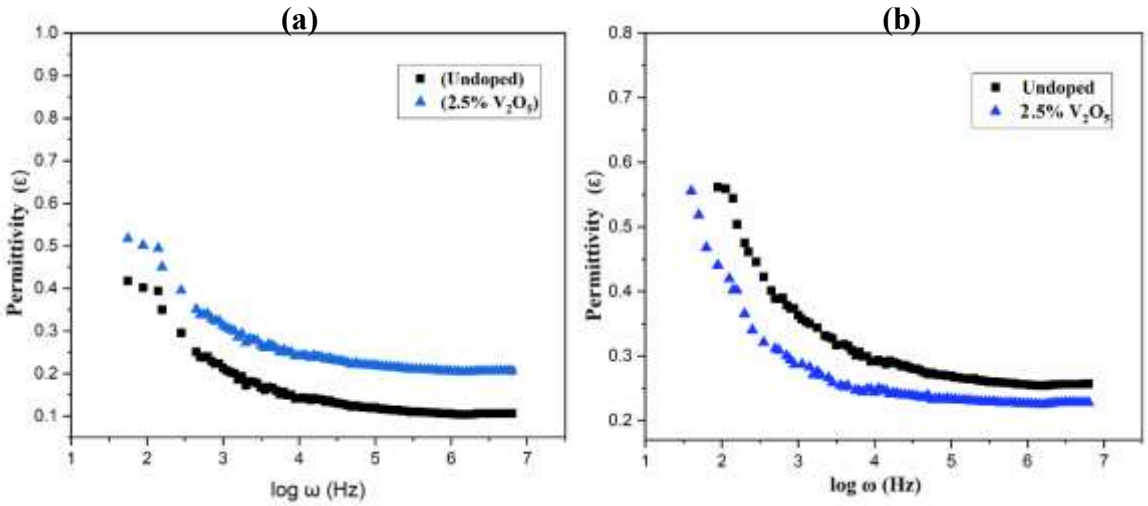

Figure 3.7 Dependence of permittivity vs frequency for base and 2.5% V_2O_5 substituted Borosilicate glass **(a)** before and **(b)** after immersion in SBF for 28 days.

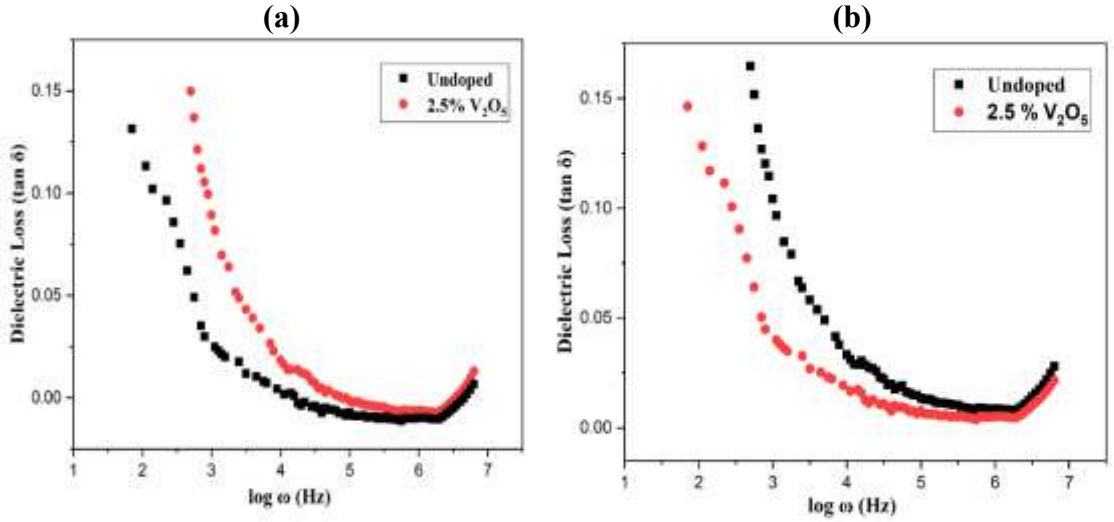

Figure 3.8 Dependence of Dielectric loss with respect to frequency of base and 2.5% V_2O_5 substituted borosilicate glass **(a)** before and **(b)** after immersion in SBF for 28 days.

The comparison of the permittivity and dielectric loss variations of the examined samples is shown in Figure 3.7(a,b) and Figure 3.8(a,b), both before and after immersion in

SBF solution. The broadening of the spectrum in the case of the post-SBF solution is clearly attributable to the existence of several processes that arise from the addition of vanadium pentoxide and the development of the HA glass complex. So, at the end, it has been determined that the electrical charges induced on biomaterial surfaces lead to improve osteopontin. These electrical properties are suitable for body tissues.

3.5 Summary:

It can be concluded that the Bioactivity of the borosilicate glass is increased after V_2O_5 substitution upto a certain level. It is observed from XRD that the nature of prepared base and substituted borosilicate glass were amorphous, as no traces of crystalline phase were observed in these bioactive glass samples. Mechanical and physical properties are being improved with an increase in V_2O_5 content. The *in-vitro* bioactivity of the base and V_2O_5 substituted (upto 4%) borosilicate glasses were increased after immersing them in SBF solution for 28 days, as observed through XRD and FTIR characterizations. SEM micrographs and EDX analysis also show the formation of HA on the surface of base and borosilicate substituted glass samples after immersion in SBF solution for 28 days. Hemocompatibility offers its compatibility with Human Blood. To test these *in-vitro* results, we check its cellular compatibility with the help of the MG-63 cell line. This shows its better biocompatibility with human bone with increasing amounts of V_2O_5 in borosilicate glass, but positive results are obtained upto 0.5% doping only. It shows low cellular viability results at higher concentrations i.e. at 2.5% and 4% V_2O_5 doping due to V_2O_5 nature. Being toxic, we also used to study V_2O_5 as doping material because the results of small amounts of V_2O_5, i.e. upto 0.5%, have very high cellular viability, so it is suitable for oosteosarcoma cases. The existence of a hydroxyapatite (HA) layer is also shown by the observed differences in electrical characteristics between base and V_2O_5 substituted samples.

Reference:

[1] L.L. Hench, The story of Bioglass®, Journal of Materials Science: Materials in Medicine, 17 (2006) 967-978

[2] L.L. Hench, Bioceramics, Journal of the American Ceramic Society, 81 (2005) 1705–1728.

[3] R.E. Youngman, Borosilicate Glasses. In Encyclopedia of Glass Science, Technology, History and Culture, (2021) 867–878. Wiley.

[4] P. Ducheyne, Q. Qiu, Bioactive ceramics: the effect of surface reactivity on bone formation and bone cell function, Biomaterials 20 (1999) 2287–2303.

[5] N. Price, S.P. Bendall, C. Frondoza, R.H. Jinnah, D.S. Hungerford, Human osteoblast-like cells (MG63) proliferate on a bioactive glass surface. Journal of Biomedical Materials Research, 37 (1997) 394–400.

[6] F.H. ElBatal, M.S. Selim, S.Y. Marzouk, M.A. Azooz, UV-vis absorption of the transition metal-doped SiO2–B2O3–Na2O glasses, Physica B: Condensed Matter, 398 (2007) 126–134.

[7] S. Ashraf, M.A. El-Morsy, N.S. Awwad, H.A. Ibrahium, Physicochemical changes of hydroxyapatite, V2O5 and graphene oxide composites for medical usages. Journal of the Australian Ceramic Society, 58 (2022) 1399–1413.

[8] G. Anto, K. Athira, N.A. Nair, T.Y. Sai, A.L. Yadav, V. Sairam, Mechanical properties and durability of ternary blended cement paste containing rice husk ash and nano silica, Construction and Building Materials, 342 (2022) 127732.

[9] T. Kokubo, H. Kushitani, S. Sakka, T. Kitsugi, T. Yamamuro, Solutions able to reproducein vivo surface-structure changes in bioactive glass-ceramic A-W3. Journal of Biomedical Materials Research, 24 (1990) 721–734.

[10] N. Pisitpipathsin, P. Kantha, S. Eitsayeam, G. Rujijanakul, R. Guo, A.S. Bhalla, K. Pengpat, Effect of BCZT on Electrical Properties and Bioactivity of 45S5 Bioglass. Integrated Ferroelectrics, 142 (2013) 144–153.

[11] A.K. Dubey, P.K. Mallik, S. Kundu, B. Basu, Dielectric and electrical conductivity properties of multi-stage spark plasma sintered HA–CaTiO3 composites and comparison with conventionally sintered materials. Journal of the European Ceramic Society, 33 (2013) 3445–3453.

[12] N.P. Rajesh, V. Athikesavan, Structural, dielectric, piezoelectric and ferroelectric properties of lead-free (1-x) Na0.5 Bi0.5 TiO3-xBaTiO3 (x=0.00, 0.04, 0.06, 0.08) ceramic. AIP Conference Proceedings, 2115 (2019) 030025.

[13] D.P. Almond, C.R. Bowen, D.A.S. Rees, Composite dielectrics and conductors: simulation, characterization and design. Journal of Physics D: Applied Physics, 39 (2006) 1295–1304.

[14] S.K. Arepalli, H. Tripathi, V.K. Vyas, S. Jain, S.K. Suman, R. Pyare, S.P. Singh, Influence of barium substitution on bioactivity, thermal and physico-mechanical properties of bioactive glass. Materials Science and Engineering: C, 49 (2015) 549-559.

[15] S. Yadav, P. Singh, R. Pyare, Synthesis, characterization, mechanical and biological properties of biocomposite based on zirconia containing 1393 bioactive glass with hydroxyapatite. Ceramics International, 46 (2020) 10442–10451.

[16] A. Ali, S.P. Singh, R. Pyare, SrO assisted 1393 glass scaffold with enhanced biological compatibility. Journal of Non-Crystalline Solids, 550 (2020) 120392.

[17] S.K. Yadav, V.K. Vyas, P. Anand, M.R. Majhi, R. Pyare, Destructive and non-destructive properties of cobalt oxide substituted 1393 bioactive glass**,** Rasayan Journal of Chemistry, 10 (2017) 935-945.

[18] A. Ali, M. Ershad, V. K. Vyas, S. K. Hira, P. P. Manna, B. N. Singh, S. Yadav, P. Srivastava, S. P. Singh, R. Pyare, Studies on effect of CuO addition on mechanical properties and in vitro cytocompatibility in 1393 bioactive glass scaffold, Materials Science and Engineering: C 93 (2018) 341–355.

[19] S-J. Park., M-K Seo, Element and Processing 18 (2011) 431–499.

[20] J-D. Zuo, S-M. Liu, Q. Sheng, Synthesis and Application in Polypropylene of a Novel of Phosphorus-Containing Intumescent Flame Retardant. Molecules, 15 (2010) 7593–7602.

[21] J. Xia, Y. Xiong, S. Min, J. Li, A review of recent infrared spectroscopy research for paper. Applied Spectroscopy Reviews. 58 (2022) 738-754.

[22] D.N. Kumar, A. Chaudhuri, F. Aqil, D. Dehari, R. Munagala, S. Singh, R.C. Gupta, A.K. Agrawal, Exosomes as Emerging Drug Delivery and Diagnostic Modality for Breast Cancer: Recent Advances in Isolation and Application. Cancers 14 (2022) 1435.

[23] V. Kushwah, S. S. Katiyar, C. P. Dora, A. Kumar Agrawal, D. A. Lamprou, R. C. Gupta, S. Jain, Co-delivery of docetaxel and gemcitabine by anacardic acid modified self-assembled albumin nanoparticles for effective breast cancer management, Acta Biomaterialia 73 (2018) 424–436.

[24] S. Das, P. Goswami, V.K. Verma, H.K. Indurthi, M. Kumar, B. Koch, D.K. Sharma, Rapid access to 7-substituted cyclo alkylamino and alkylamino analogues of 4-methylcoumarin reveals surprising emitters, Dyes and Pigments, 217 (2023) 111407.

[25] M.A. Azooz, T.H.M.A. Aiad, H. Elbatal, G. Eltabii, Characterization of bioactivity in transition metal doped-borosilicate glasses by infrared reflection and dielectric studies, Indian Journal of Pure & Applied Physics, 46 (2008) 880-888.

[26] X. Lu, R. Sun, L. Huang, J.V. Ryan, J.D. Vienna, J. Du, Effect of vanadium oxide addition on thermomechanical behaviours of borosilicate glasses: Toward development of high crack resistant glasses for nuclear waste disposal, Journal of Non-Crystalline Solids, 515 (2019) 88–97.

[27] U. Pantulap, M. Arango-Ospina, A.R. Boccaccini, Bioactive glasses incorporating less-common ions to improve biological and physical properties. Journal of materials science, Materials in medicine, 33 (2021) 3.

[28] S. Prasad, V.K. Vyas, R. Pyare, K. Mani, Study of physical and mechanical properties of BG/HA/TiO2 biocomposite for bone implantation. International Journal of Advanced Research, 4 (2016) 268–279.

[29] S. K. Yadav, S. Ray, M. Ershad, V. K. Vyas, S. Prasad, A. Ali, S. Yadav, M. R. Majhi, R. Pyare, Development of Zirconia Substituted 1393 Bioactive Glass for Orthopaedic Application, Oriental Journal of Chemistry 33 (2017) 2720–2730.

[30] M.A. Ur Rehman, F.E. Bastan, A. Nawaz, Q. Nawaz, A. Wadood, Electrophoretic deposition of PEEK/bioactive glass composite coatings on stainless steel for orthopedic applications: an optimization for in vitro bioactivity and adhesion strength, The International Journal of Advanced Manufacturing Technology, 108 (2020) 1849–1862.

[31] K. Singh, I. Bala, V. Kumar, Structural, optical and bioactive properties of calcium borosilicate glasses. Ceramics International, 35 (2009) 3401–3406.

[32] A.K. Jonscher, The ‘universal’ dielectric response. Nature, 267 (1977) 673–679.

[33] R. Halder, P. Sengupta, V. Sudarsan, C.P. Kaushik, G.K. Dey, Investigating the effect of V2O5 addition on sodium barium borosilicate glasses, 1731 (2016) 070005.

[34] N. Singh, P. Singh, Cu (i) substituted wurtzite ZnO: a novel room temperature lead free ferroelectric and high- κ giant dielectric. RSC Advances, 10 (2020) 11382–11392.

[35] S. Yadav, S. Majumdar, A. Akher, S. Krishnamurthy, P. Singh, R. Pyare, In-vitro Analysis of Bioactivity, Hemolysis, and Mechanical Properties of Zn Substituted Calcium Zirconium Silicate (Baghdadite), Ceramics International 47 (2021) 16037-16053.